

Lipodisqs for eukaryote lipidomics with retention of viability: sensitivity and resistance to *Leucobacter* infection linked to *C.elegans* cuticle composition

Juan F. Bada Juarez¹, Delia O'Rourke¹, Peter J. Judge¹, Li C. Liu¹, Jonathan Hodgkin^{1*} and Anthony Watts^{1*}

¹Department of Biochemistry, University of Oxford, South Parks Road, OX1 3QU, Oxford

* corresponding authors: anthony.watts@bioch.ox.ac.uk, jonathan.hodgkin@bioch.ox.ac.uk

Abstract

Lipodisq™ nanoparticles have been used to extract surface lipids from the cuticle of two strains (wild type, N2 and the bacterial-resistant strain, *agmo-1*) of the *C. elegans* nematode without loss of viability. The extracted lipids were characterized by thin layer chromatography and MALDI-TOF-MS. The lipid profiles differed between the two strains. The extracted lipids from the bacterial resistant strain, *agmo-1*, contained ether-linked (O-alkyl chain) lipids, in contrast to the wild type strain which contained exclusively ester (O-acyl) linked lipids. This observation is consistent with the loss of a functional alkylglycerol monooxygenase (AGMO) in the bacterial resistant strain *agmo-1*. The presence and abundance of other lipid species also differs between the wild-type N2 and *agmo-1* nematodes, suggesting that the *agmo-1* mutant strain attempts to compensate for the increase in ether-linked lipids by modulating other lipid-synthesis pathways. Together these differences not only affect the fragility of the cuticle and the buoyancy of the worm in aqueous buffer, but also interactions with surface-adhering bacteria. The much greater chemical stability of O-alkyl, hydrolysable linked lipids compared with non-hydrolysable O-acyl linked lipids, may be the origin of the bacterial resistance of the *agmo-1* strain, providing a more resilient cuticle for the nematode. Additionally, we show that lipid extraction with a polymer of styrene and maleic acid (SMA) provides a viable route to lipidomics studies with minimal perturbation of the organism.

1. Introduction

C. elegans has been a successful model organism for the study of both animal development and behaviour for more than 50 years^{1,2}. The genome was the first from a multicellular organism to be sequenced³ and their simplicity makes them a perfect system for studies of gene expression, ageing, development and the nervous system⁴. The *C. elegans* 'exoskeleton'⁵, the cuticle, which forms a barrier between the external environment and the worm epidermis, is poorly characterized. The cuticle has an important role in *C. elegans* biology, as it maintains body shape while permitting locomotion and nutrition, and also offers protection against bacterial and fungal parasites⁶.

Previously, we described the isolation of two new *Leucobacter* bacterial pathogens of *Caenorhabditis*, discovered co-infecting a wild isolate collected in Cape Verde⁷. The interactions of these bacteria with *C. elegans* revealed unusual mechanisms of pathogenic attack: one pathogen, Verde1, traps swimming nematodes by sticking their tails together, resulting in the formation of "worm-star" aggregates, in which worms were killed and degraded; the other pathogen, Verde2, kills worms by a different mechanism associated with rectal infection. Both infections require the attachment of bacteria to the cuticle for their pathogenic effects⁷.

Genetic screens identified many distinct mutant worms that were resistant to lethal *Leucobacter* Verde2 infection. These mutants alter the chemical properties of the worm surface, preventing Verde2 attachment and also affecting movement, sensitivity to bleach and the binding of lectins. The Verde2-resistant mutants are however hypersensitive to *Leucobacter* Verde1 infection. Further genetic suppressor screens to reverse the lethal sensitivity of these mutants to Verde1 suggested a common mechanism involved in suppression of Verde1 infection, identified as the loss of the pathway required for the degradation of ether lipids. Many independent suppressor mutations were found in the gene encoding alkylglycerol monooxygenase (AGMO), a metabolic enzyme solely responsible for the degradation of ether-linked lipids^{8,9}, or in enzymes required for the synthesis of its essential cofactor tetrahydrobiopterin^{8,10}. This striking reciprocal sensitivity and resistance to Verde1 and Verde2 may reflect the fact that these pathogens were isolated as a co-infection of wild-type

Caenorhabditis, suggesting that the worms may have developed a trade-off relationship between sensitivity and resistance to the two pathogens⁷.

The finding that loss of the ether lipid degradation pathway confers resilience to Verde1 infection, suggested that changes in the lipid content of the *C. elegans* cuticle are responsible for altering the susceptibility to the Verde1 and Verde2 infection mechanisms⁷. Here we complement the genetic analysis of *C. elegans* surface with a biochemical analysis of the cuticle lipidome, both in mutants that demonstrate resistance to Verde1 infection and in wild-type worms.

The *C. elegans* cuticle is secreted by the underlying epithelial cells and is regenerated entirely following moulting at four larval growth stages (L1-4). It is thought that the thickness of the cuticle, as well as its protein and lipid composition, change at every larval stage and may vary in response to the environment^{4,5}. The cuticle consists of several layers, the outermost being the surface coat, which is covered by glycoproteins and has a net negative charge at neutral pH, due to the presence of sugar-sulphate moieties⁶. This outermost layer is likely to play an important role in locomotion and may prevent the adhesion of microbes to the nematode surface⁵. *C. elegans srf* mutants, with an altered carbohydrate epitope expression profile on the coat, have a weakened cuticle and modified bacterial adherence⁵. Other additional *bus* (Bacterially UnSwollen) mutants show similar phenotypes, including modified surface lectin binding¹¹.

Below the hydrophilic surface coat, the epicuticle contains both glycoproteins and lipids, including non-polar species such as steroids (particularly cholesterol), polar lipids such as PC and PE and some glycolipids, which appear to have important roles in the immune response^{6,12}. With the exception of the epicuticle and the surface coat, the cuticle is predominantly made of collagen and its derivatives (cross-linked and collagen-like molecules)¹³. The epicuticle of the parasitic nematode *Trichinella spiralis*, is mainly composed of PC, PE and PG and has lipids arranged in an inside-out cylindrical configuration, in which the hydrophilic headgroups point inwards, exposing the hydrophobic tails to the rest of the cuticle¹⁴.

Lipid mobility in the cuticles of several nematode species is restricted compared to a typical plasma membrane^{4,15}. The presence of lipids in the epicuticle of other nematodes has been assessed by fluorescent probes and lipase treatment^{4,5,16,17} and the flexibility and resistance to chemical and physical stresses have been attributed to the presence of some waxes and/or glycolipids (ascarosides¹⁷). Conversely, proteins in the epicuticle have been shown to diffuse quickly, which is attributed both to weak ionic interactions with lipids and also due to their distribution in membrane domains containing neutral lipids, in which they can diffuse freely^{4,15}.

We set out to identify the components of the nematode surface in order to understand how defects in lipid metabolism change the surface of *C. elegans* and thereby alter patterns of bacterial adherence. We focused on differences between wild-type N2 worms and the most frequently identified Verde1 suppressor mutant, *agmo-1*, which lacks alkylglycerol monooxygenase (AGMO)^{8,9}. By disrupting the metabolic pathways responsible for lipid synthesis⁹, loss of the enzyme might alter the sensitivity towards bacterial pathogens through a destabilization of the cuticle. While the total lipidome of *C. elegans* has been partially analysed using imaging, genetic and biochemical techniques^{16,18–20}, the characterization the of *C. elegans* surface has been limited⁶, owing to the difficulty of selectively extracting lipids from the cuticle, without contamination from other cellular membranes in the worm.

SMA (a hydrolysed co-polymer of styrene and maleic anhydride) has recently been shown to be able to simultaneously extract both lipids and proteins from biological membranes. The polymer extracts lipids non-selectively, preserving protein structure and activity^{21–25}. The resulting nanoparticles (commonly termed Lipodisq or SMALPs) have also been used for structural characterization by cryo-EM^{26,27} and X-ray crystallography²⁸. Several membrane proteins including ion channels²⁹ and GPCRs^{30,31} have been studied and characterized from different organisms^{32–35} and some proteomics and lipidomics experiments have been performed using SMALPs by hydrogen-deuterium exchange mass spectrometry and LC-MS/MS^{36,37}.

Here, SMA polymer is used to extract the lipids present in the nematode cuticle of *C. elegans* wild-type (N2) and *agmo-1* strains. We characterise the surface lipids from the wild-type and mutant strains of *C. elegans* using MALDI-TOF-MS. Our aim is to identify and understand the

molecular differences in cuticle composition and structure, which underpin the different phenotypes of the wild-type and surface mutant nematodes.

2. Material and methods

2.1. *C. elegans* culture

The N2 (wild-type) and *agmo-1* (strain CB7014, genotype *agmo-1(e3016)*) nematodes were grown on nematode growth media plates². The generations were synchronized in order to obtain a homogeneous population prior to SMA polymer addition.

2.2. Formation of Lipodisq nanoparticles

SMA polymer containing a molar ratio of styrene:maleic acid of 3:1 was supplied by Malvern Cosmeceutics Ltd (Malvern, UK). Synchronised populations of worms were harvested by washing the media plates with 10 mM Tris 5 mM NaCl pH 8 followed by three rounds of centrifugation (2500g, 2 minutes, 4°C). An SMA solution (25% w/v in 50 mM Tris buffer pH 8) was added to the washed worms at a final concentration of 12.5% v/v in 50 mM Tris buffer pH 8 and incubated for 30 minutes at 30-40 °C. The sample was centrifuged, and the supernatant was kept for further analysis.

2.3. Dynamic light scattering measurement

The size of the Lipodisq nanoparticles, generated by lipid extraction by SMA, was measured by Dynamic Light Scattering at 633 nm using a Malvern Zetasizer Nano S instrument with a disposable cuvette. Data were processed using Malvern Zetasizer software.

2.4. Viability test of worms after SMA treatment

Worms were deposited onto a freshly seeded OP50 NGM plate and left at room temperature. The recovery was assessed from the percentage of worms that crawled across the OP50 making visible tracks. Plates were observed under a dissecting microscope after 1, 2, 4 and 24 hours, and were compared to those with nematodes that had not been exposed to SMA.

2.5. Lipids extraction from Lipodisq nanoparticles

Lipids were extracted from the Lipodisq samples according to the method of Bligh and Dyer³⁸. Briefly, 200 µL Lipodisq-containing sample was mixed vigorously for 1 h, with 2 mL

chloroform/methanol (2:1 v/v). Phase separation was achieved by adding 1 mL of ddH₂O water. The extract was left for 10 minutes at room temperature and then centrifuged (1,000g, 10 min) and the lower phase was retrieved washed twice with a methanol/water mix (1:1 v/v) and dried under a stream of N₂ gas.

2.6. Matrix-assisted laser desorption ionization mass spectrometry

Water and DHB matrix were spotted onto a MALDI plate (MTP 384 Polished Steel TF Targets) and allowed to dry at room temperature. Lipids were resuspended in chloroform/methanol mixture (2:1 v/v), deposited above the dried matrix and allowed to dry at room temperature. MALDI TOF mass spectra were acquired using a Bruker Ultraflex TOF/TOF operating in linear positive ion mode. MALDI laser intensity was selected to provide optimal intensity and resolution of acquired mass spectra. External calibration was performed using protein standards and some lipids standards, which were analysed under identical conditions. The identification of lipid was performed using LIPID MAPS online searching tools³⁹ and data analysis was performed using the Thermo XCalibur (ThermoFisher) processing software and plotted in Prism (GraphPad software).

3. Results

To determine the cuticle lipid composition of both wild-type (N2) and mutant (*agmo-1*) *C. elegans*, nematodes were incubated with SMA polymer. Both the time of incubation and temperature were adjusted to ensure that both wild-type and mutant worms recovered after the SMA treatment as shown in Figure 1. The best conditions for the SMA extraction of the nematode surface were found to be a temperature of between 30°C and 40°C and an incubation time of 30 to 60 minutes.

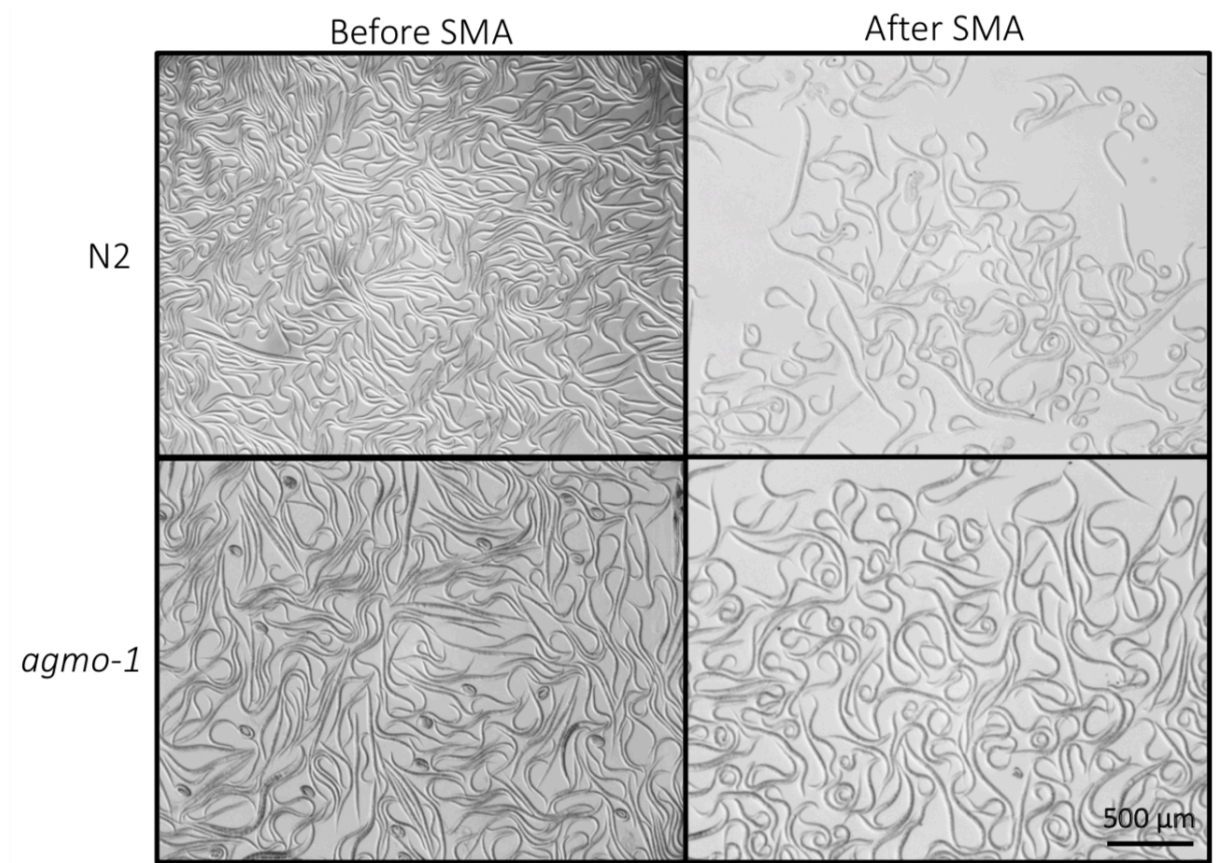


Figure 1 Synchronised worms before and after addition of SMA polymer. The viability and integrity of the worms was not affected as shown here.

After incubation, the SMA-worm suspension was centrifuged, the supernatant was collected and DLS measurements were performed to verify Lipodisq nanoparticle formation (Figure 2; Table 1). DLS data show that Lipodisqs were present in the supernatant (peak at 4-6 nm),

although some excess SMA was still present in the N2 strain sample (identified by the peak at 1.3 nm. The *agmo-1* mutant strain did not contain any excess SMA, despite the fact that the same number of worms was used to perform this experiment as for the wild type. A viability test showed that more than 95% of the worms survived the SMA incubation (data not shown).

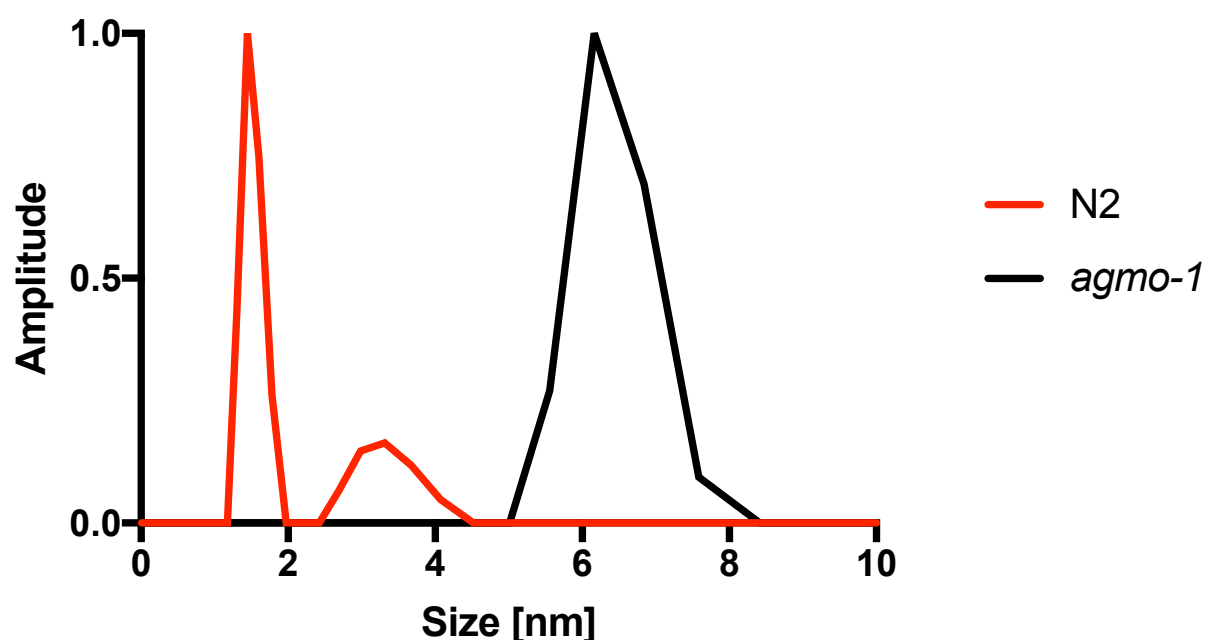


Figure 2 Dynamic light scattering experiment showing the different sizes obtained for both strains after SMA addition.

Table 1 DLS data for the SMA nanoparticles from the wild-type (N2) and the mutant strain (*agmo-1*)

Peak	N2	<i>agmo-1</i>
SMA polymer	1.5 ± 0.1 nm	-
Lipodisq nanoparticles	3.3 ± 0.4 nm	6.4 ± 0.4 nm

After the DLS analysis, the lipid composition of the Lipodisq nanoparticles from both nematode strains were investigated. Lipids were extracted by following the method of Bligh and Dyer³⁸ and were analysed by thin layer chromatography (TLC) (Figure SI.1), as described previously^{29,36}. Lipid headgroups were identified by their retention factor (R_f) values (Table 2). Ceramides, commonly found in the skin of mammals⁴⁰ in which they appear to play a role in the organisation of other lipids⁴¹, are found in both wild type and mutant worms, and their appearance is consistent with the slow lipid diffusion rates previously reported in the cuticle^{4,15,42}. Also present in both strains were cerebroside (Cb) and lyso-phosphatidylcholine (LPC). For the N2 strain, lipids such as phosphoethanolamine (PE), lyso-phosphatidylglycerol

(LPG), sphingosine/sphingomyelin (SM) and lyso-phosphatidylserine (LPS) were found, whereas in the mutant *agmo-1*, phosphatidyl-N-monomethylethanolamine (PMME), cardiolipin (CL) and PG were found. Also, some lipid species are not able to migrate in the chosen solvent mixture, and this might indicate the presence of highly charged species as speculated by Blaxter and colleagues⁶.

Table 2 The different lipids identified (with their retention factors in brackets) by TLC and compared to the literature. ND, unidentified lipids.

N2	<i>agmo-1</i>	N2 from Blaxter ⁶		
PE (0.79)	PMME (0.71)	PI (0.09)	Glycerophosphocholines	PC (LPC for lyso species)
LPG (0.54)	CL (0.67)	ND (0.24)	Glycerophosphoethanolamines	PE (LPE for lyso species)
SM (0.28)	PG (0.6)	PC (0.38)	Glycerophosphoserines	PS (LPS for lyso species)
LPS (0.18)	-	PE (0.5)	Glycerophosphoglycerols	PG (LPG for lyso species)
CE (1)		ND (0.61)	Glycerophosphates	PA (LPA for lyso species)
Cb (0.94)		Sterol (0.9)	Glycerophosphoinositols	PI (LPI for lyso species)
LPC (0.22)		ND (1)	Glycerophosphoglycerophosphoglycerols (Cardiolipins)	CL
			Monoradylglycerolipids	MG
			Diradylglycerolipids	DG
			Triradylglycerolipids	TG
			Digalactosyldiacylglycerols	DGDG
			Sulfoquinovosyldiacylglycerols	SQDG
			Ceramides/Sphingoid bases	Cer/Sph
			Hexosyl ceramides	HexCer
			Mannosyl-PI-ceramides	MIPC
			Mannosyl-di-PI-ceramides	M(IP) ₂ C
			Lactosyl ceramides	LacCer
			Sulfatides	SHexCer
			Wax esters	WE
			Cholesteryl esters	CE
			Fatty acids	FA
			Lyso-phosphatidylinositol-monophosphate	LPIP

TLC is not able to distinguish between ester- and ether-linked lipids with the same headgroup and MALDI-TOF MS was therefore used to assist in the identification of some of the lipids present. As some of these lipids have a mass below 1 kDa, the instrument was calibrated using low molecular weight protein standards in addition to lipids such as DMPC, POPC, DOPC and POPG. Moreover, as the 500 Da to 1000 Da mass range is difficult to study due to the noise peaks produced by the matrix, a control experiment including the recording of mass spectra of matrix-only spots was performed (data not shown) and the peaks of this matrix-only experiment were subtracted from the Lipodisq sample experiments. Another control was performed which includes the removal of the peaks coming from the OP50 bacterial source lipids extracted using SMA. Matrix-only peaks were subtracted from the mass spectra of N2 and *agmo-1*. The mass spectra for the N2 and *agmo-1* after removal of both the matrix and OP50 lipids peaks are shown in Figure 4.

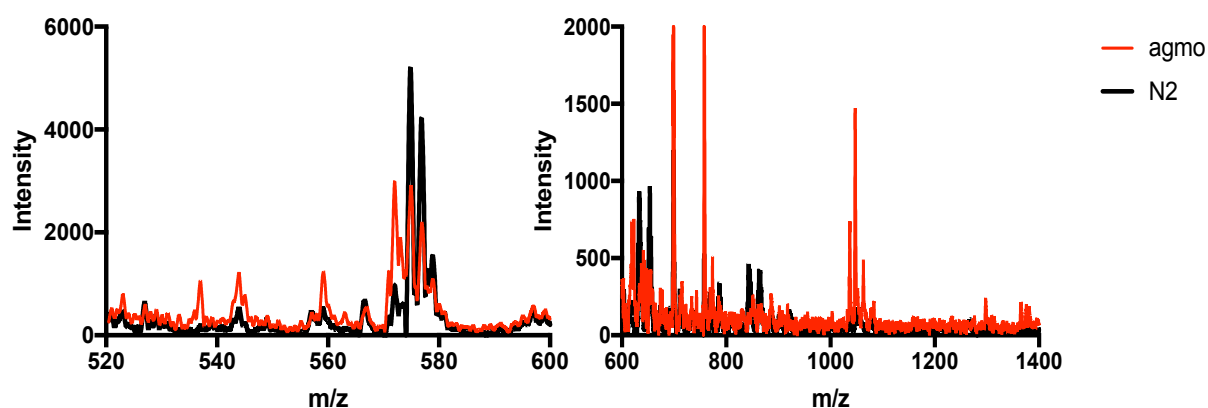


Figure 3 MALDI-MS spectra at different range exhibiting different peaks. In red the *agmo-1* mutant and in dark the wild-type. Some differences are observed especially in the 600-1200 *m/z* region.

Lipid peaks were determined with an intensity above 500 (signal-to-noise ratio > 2) and peaks were assigned (Table 3). Identification of lipids was performed using the LipidMAPS website³⁹ with a mass tolerance of ± 0.1 *m/z*. All peaks were considered as possible ion adducts with potassium, sodium, with a possible loss of water and as singly and doubly charged, (MALDI primarily generates sodium and potassium adducts of singly or doubly charged species⁴³). As expected, no ether lipids (coloured red in Table 3), were identified in the N2 wild-type strain, however up to two ether lipid species were identified in the *agmo-1* mutant.

Some lipid species (rendered in green in Table 3) are observed in both the N2 and *agmo-1* samples, including PA, PI, sulfoquinovosyldiacylglycerol (SQDG) and lyso-phosphatidylinositol-monophosphate (LPIP). In addition to these lipids, the N2 strain has some additional lipid types which include PS and MIPC.

Table 3 The different lipids identified in SMA extracts using the LipidMAPS website³⁹. In red the lipids which have been identified as ether-linked lipids (with O- indicating alkyl ether-linked lipids and P- indicating alkneyl-ether (plasmalogen) lipids) and in green lipids which are shared between the wild-type and mutant strain. In orange, the different ceramides with d and t designating the shorthand notation for sphingolipids and refer to 1,3-dihydroxy and 1,3,4-trihydroxy long-chain bases.

<i>agmo-1</i>				
Mass (Da)	Abbreviation	Full name	Headgroup charge	Chain length and unsaturation
1539,587	TG	Triradylglycerolpid	0	99:0
1385,993	DGDG	Digalactosyldiacylglycerol	0	65:7
1369,024	PIP	Glycerophosphoinositol monophosphate	2-	65:1
1366,886	CL or PIP	Cardiolipin or Glycerophosphoinositol monophosphate	2-	66:7 or 66:8
1290,895	PIP	Glycerophosphoinositol monophosphate	2-	60:5
1279,758	PIP	Glycerophosphoinositol monophosphate	2-	58:7
1277,554	M(IP) ₂ C	Mannosyl-di-glycerophosphoinositol-ceramide	2-	d46:3
1165,738	SQDG	Sulfoquinovosyldiacylglycerol	1-	57:9
1158,823	PE	Glycerophosphoethanolamine	0	64:10
1148,848	LacCer	Lactosyl ceramide	0	t50:0
1141,55	M(IP) ₂ C	Mannosyl-di-PI-ceramide	2-	d31:2
1134,746	PC	Glycerophosphocholine	0	58:12
1120,828	PC or PE	Glycerophosphocholine or Glycerophosphoethanolamine	0	58:8 or 61:8
1107,787	PS	Glycerophosphoserine	1-	60:10
1106,841	LacCer	Lactosyl ceramide	0	d50:2
1087,602	PIP	Glycerophosphoinositol monophosphate	2-	46:8
1006,738	DGDG	Digalactosyldiacylglycerol	0	39:1
947,71	PA, PG or TG	Glycerophosphoglycerol	1-	O-53:6, P-50:6, 58:11
946,785	TG	Triradylglycerolpids	0	58:9
888,844	DG, TG(O) or TG(P)	Diacylglycerol, Triacylglycerol	0	54:3, O-54:3, P-54:2
850,358	PIP	Glycerophosphoinositol monophosphate	2-	27:2
837,42	SQDG	Sulfoquinovosyldiacylglycerols	1-	33:5
824,388	LPIP	Lyso-Glycerophosphoinositol monophosphate	2-	25:1
811,422	LPIP	Lyso-Glycerophosphoinositol monophosphate	2-	29:3
760,465	ShexCer	Sulfatides hexosyl ceramide	1-	d31:1
751,324	SQDG	Sulfoquinovosyldiacylglycerol	1-	27:6
703,549	HexCer	Hexosylceramide	0	t32:2
698,689	CE or WE	Ceramide or Wax ester	0	20:0 or 47:5
655,376	PA	Glycerophosphate	1-	30:2
653,3	SQDG	Sulfoquinovosyldiacylglycerol	1-	24:6
603,446	PI	Glycerophosphoinositol	1-	57:0
576,466	PG	Glycerophosphoglycerol	1-	62:4
566,379	PI	Glycerophosphoinositol	1-	55:9

N2				
Mass (Da)	Abbreviation	Full name	Headgroup charge	Chain length and unsaturation
996,704	PS	Glycerophosphoserine	1-	48:1
811,422	LPIP	Lyso-Glycerophosphoinositol monophosphate	2-	29:3
760,332	MIPC	Mannosyl-PI-ceramide	1-	t18:0
655,376	PA	Glycerophosphate	1-	30:2
653,3	SQDG	Sulfoquinovosyldiacylglycerol	1-	24:6
566,379	PI	Glycerophosphoinositol	1-	55:9

4. Discussion

The SMA lipid extraction method used here, appears to be milder than protocols involving detergent or organic extractions⁶, and the fact that 95% of the nematodes are viable after treatment with SMA, suggests that the integrity of the cell membranes in the *C. elegans* body is not severely compromised, and that the polymer primarily extracts lipids from the cuticle.

The DLS data suggest that the lipid extraction from the worms by SMA, results in the formation of Lipodisq nanoparticles, with diameters measured in the range 6 nm – 25 nm (Table 1), similar to those previously reported^{22–24,44,45}. The sizes of the particles formed, differs between the N2 and *agmo-1* strains, consistent with a difference in lipid content and also might indicate differences in protein content. Additionally, the N2 cuticle is more resistant to SMA treatment, in agreement with earlier studies which indicate that the *agmo-1* cuticle is more fragile⁹. The accumulation of ether lipids may compromise the stability of the *agmo-1* cuticle, despite its ability to prevent Verde1 attachment to *C. elegans* surface.

Identification of lipid headgroups was carried by TLC and some retention factors measured in previous publications⁶ are similar to our data and can be identified⁴⁶. Therefore, the $R_f=0.24$ could be LPC-type lipids and the $R_f=0.61$, could be PG-type lipids. Some of the lipids found in the Lipodisq extraction were also identified by Blaxter and colleagues, such as PE and ceramides, however we were unable to identify PC or PI from in our data (Table 2). The presence of SQDG and ceramide-type lipids (Figure 3 and Table 3) is consistent with literature, especially for the sulfonated lipids, which are responsible for the negative charge on the cuticle. All of the lipids identified by the TLC analysis are lipid species expected from previous genetic studies of *C. elegans*¹⁶.

Since the *agmo-1* mutant lacks alkylglycerol monooxygenase (AGMO), which cleaves the ether bond of alkylglycerols, we expect to observe some differences in the abundance of ether-linked lipids in the mutant. Compared to the wild-type strain, more lipids were observed and identified for the *agmo-1* mutant, as seen by the TLC (Figure 3). The lipids highlighted (in red in Table 3) are ether-linked lipid species, which have been speculated to accumulate at the cuticle surface due to the lack of the AGMO enzyme. The literature suggest that sulfatides, PE and PI have the

lowest detectability threshold⁴⁷. Therefore their identification in this experiment, may mean that the sample contains a high amount of these lipids, which is not surprising as PI and sulfatides lipids have been suggested to regulate the cuticle surface charge⁶.

The accumulation of some ether-linked lipids at the cuticle surface of the mutant, may prevent bacterial adherence by masking binding targets on the worm surface. The *agmo-1* nematodes float on aqueous buffer (unlike wild-type worms) consistent with an increased abundance of ether-linked lipids and waxes, both of which have been reported to affect buoyancy⁴⁸. The wild-type cuticle also contains greater relative abundance of negatively charged lipid headgroups, which are diluted by the ether-linked lipids and ceramides in the *agmo-1* mutant, which may also explain the differences in the apparent ease of solubilisation of the cuticle lipids by the negatively charged SMA polymer.

Surprisingly we also observe some ester-linked lipid species in the *agmo-1* mutant which are not found in the N2 strain. We propose that a compensation mechanism is effected, by which results in the upregulation of other lipid synthesis pathways and the more heterogeneous lipid composition of the mutant cuticle. A similar phenomenon has been observed in murine macrophage-like cells, in which a decrease in AGMO activity (and increase in free alkylglycerol lipid types) resulted in widespread changes in the cell lipidome, including changes in the abundance of glycosylated ceramides and cardiolipin¹⁰. In our case, we found several glucosylceramides in the *agmo-1* mutant, which have been suggested to be located in the nematode's cuticle⁴⁹, some tri- and diacylglycerols and only one cardiolipin¹⁰. We suggest that the protein composition also differs as a result of changes in lipid-protein interactions.

Ether lipid-deficient strains in *C. elegans* accumulate high levels of stearic acid (18:0) in several types of ester-linked lipid, presumably to compensate for the reduced rigidity that would be conferred by the ether lipids⁵⁰. It is striking that longer chain length lipids with high molecular weights are observed in the *agmo-1* mutant but not the N2 strain. The wild-type cuticle has a less diverse lipidome, and the lipids present generally have shorter acyl chain lengths than the mutant.

5. Conclusion

We have demonstrated that lipid extraction by SMA may be used to study the lipidome of the *C. elegans* cuticle. We have shown that SMA can be used on living organisms without affecting their viability, compared to harsher lipid extraction methods such as those requiring organic solvents (Figure 1). We have identified an accumulation of ether-linked lipids in the *agmo-1* mutant nematode cuticle, which is consistent with the deletion of a functional alkylglycerol monooxygenase (AGMO) in this strain⁹. The presence and abundance of other lipid species also differ between the wild-type N2 and *agmo-1* worms, suggesting that the mutant strain attempts to compensate for the increase in ether-linked lipids by modulating other lipid-synthesis pathways. Together these differences not only affect the fragility of the cuticle⁹ and the buoyancy of the worm in aqueous buffer, but also the interactions between the exoskeleton and surface-adhering bacteria⁹.

Acknowledgments

We thank Dr Holger Kramer for access to MS equipment and Peter Fisher for technical assistance. This study was partly funded by MRC grant MR/J001309/1 and a Faucett Catalyst Grant (to JH). We also thank Malvern Cosmeceutics (Steve Tonge and Andy Harper) for their continued support and supply of SMA polymer.

References

1. J. Sulston and J. Hodgkin. *The Nematode Caenorhabditis elegans*. (Cold Spring Harbor Laboratory, 1988).
2. Brenner, S. The genetics of *Caenorhabditis elegans*. *Genetics* (1974). doi:10.1002/cbic.200300625
3. Bloom, F. E. Staying afloat on the seas of data. *Science* (80-.). **282**, 1989 (1998).
4. Riddle, D. L., Blumenthal, T. & Meyer, B. J. C. *elegans*. (Cold Spring Harbor, 1997).
5. Page, A. The cuticle. *WormBook* 1–15 (2007). doi:10.1895/wormbook.1.138.1
6. Blaxter, M. L. Cuticle surface proteins of wild type and mutant *Caenorhabditis elegans*. *J. Biol. Chem.* **268**, 6600–9 (1993).
7. Hodgkin, J., Félix, M.-A., Clark, L. C., Stroud, D. & Gravato-Nobre, M. J. Two *Leucobacter* Strains Exert Complementary Virulence on *Caenorhabditis* Including Death by Worm-Star Formation. *Curr. Biol.* **23**, 2157–2161 (2013).
8. Watschinger, K. & Werner, E. R. Alkylglycerol monooxygenase. *IUBMB Life* **65**, 366–372 (2013).
9. Loer, C. M. *et al.* Cuticle integrity and biogenic amine synthesis in *Caenorhabditis elegans* require the cofactor tetrahydrobiopterin (BH4). *Genetics* **200**, 237–253 (2015).
10. Watschinger, K. *et al.* Tetrahydrobiopterin and alkylglycerol monooxygenase substantially alter the murine macrophage lipidome. *Proc. Natl. Acad. Sci.* **112**, 2431–2436 (2015).
11. Gravato-Nobre, M. J. *et al.* Multiple genes affect sensitivity of *Caenorhabditis elegans* to the bacterial pathogen *Microbacterium nematophilum*. *Genetics* **171**, 1033–1045 (2005).
12. Chisholm, A. D. & Xu, S. The *Caenorhabditis elegans* epidermis as a model skin. II: differentiation and physiological roles. *Wiley Interdiscip. Rev. Dev. Biol.* **1**, 879–902 (2012).
13. Johnstone, I. L. The cuticle of the nematode *Caenorhabditis elegans*: A complex collagen structure. *BioEssays* **16**, 171–178 (1994).
14. Gounaris, K., Smith, V. P. & Selkirk, M. E. Structural organisation and lipid composition of the epicuticular accessory layer of infective larvae of *Trichinella spiralis*. *Biochim. Biophys. Acta - Biomembr.* **1281**, 91–100 (1996).
15. L, P., Kusel J R, S. H. V & W., K. M. Biophysical properties of the nematode surface. *Parasit. nematodes---Membranes, antigens genes* (1991).
16. Witting, M. & Schmitt-Kopplin, P. The *Caenorhabditis elegans* lipidome: A primer for lipid analysis in *Caenorhabditis elegans*. *Arch. Biochem. Biophys.* **589**, 27–37 (2016).
17. Lee, D. L. *The biology of the nematodes*. (CRC Press, 2002).
18. Matyash, V., Liebisch, G., Kurzchalia, T. V., Shevchenko, A. & Schwudke, D. Lipid extraction by methyl- *tert* -butyl ether for high-throughput lipidomics. *J. Lipid Res.* **49**, 1137–1146 (2008).
19. Zhang, R. & Hou, A. Host-Microbe Interactions in *Caenorhabditis elegans*. *ISRN Microbiol.* **2013**, 1–7 (2013).
20. Shi, S., Luke, C. J., Miedel, M. T., Silverman, G. A. & Kleyman, T. R. Activation of the *caenorhabditis elegans* degenerin channel by shear stress requires the MEC-10 subunit. *J. Biol. Chem.* **291**, 14012–14022 (2016).
21. Scheidelaar, S. *et al.* Molecular Model for the solubilization of membranes into nanodisks by styrene maleic acid copolymers. *Biophys. J.* **108**, 279–290 (2015).

22. Dörr, J. M. *et al.* The styrene–maleic acid copolymer: a versatile tool in membrane research. *Eur. Biophys. J.* **45**, 3–21 (2016).
23. Esmaili, M. & Overduin, M. Membrane biology visualized in nanometer-sized discs formed by styrene maleic acid polymers. *Biochim. Biophys. Acta - Biomembr.* **1860**, 257–263 (2018).
24. Lee, S. C. *et al.* A method for detergent-free isolation of membrane proteins in their local lipid environment. *Nat. Protoc.* **11**, 1149–1162 (2016).
25. Dominguez Pardo, J. J. *et al.* Solubilization of lipids and lipid phases by the styrene–maleic acid copolymer. *Eur. Biophys. J.* **46**, 91–101 (2017).
26. Parmar, M. *et al.* Using a SMALP platform to determine a sub-nm single particle cryo-EM membrane protein structure. *Biochim. Biophys. Acta - Biomembr.* **1860**, 378–383 (2018).
27. Sun, C. *et al.* Structure of the alternative complex III in a supercomplex with cytochrome oxidase. *Nature* **557**, 123–126 (2018).
28. Broecker, J., Eger, B. T. & Ernst, O. P. Crystallogenes of Membrane Proteins Mediated by Polymer-Bounded Lipid Nanodiscs. *Structure* **25**, 384–392 (2017).
29. Dörr, J. M. *et al.* Detergent-free isolation, characterization, and functional reconstitution of a tetrameric K⁺ channel: The power of native nanodiscs. *Proc. Natl. Acad. Sci.* **111**, 18607–18612 (2014).
30. Jamshad, M. *et al.* G-protein coupled receptor solubilization and purification for biophysical analysis and functional studies, in the total absence of detergent. *Biosci. Rep.* **35**, 1–10 (2015).
31. Logez, C. *et al.* Detergent-free Isolation of Functional G Protein-Coupled Receptors into Nanometric Lipid Particles. *Biochemistry* **55**, 38–48 (2016).
32. Gulati, S. *et al.* Detergent-free purification of ABC (ATP-binding-cassette) transporters. *Biochem. J.* **461**, 269–278 (2014).
33. Postis, V., Rawson, S., Mitchell, J., ... S. L.-... et B. A. (BBA & 2015, undefined. the Use of Sma Lipid Particles As a Novel Membrane Protein Scaffold for Structure Study By Negative Stain Em.Pdf. *Elsevier* **1848**, 496–501 (2015).
34. Swainsbury, D. J. K. *et al.* Probing the local lipid environment of the Rhodobacter sphaeroides cytochrome bc₁ and Synechocystis sp. PCC 6803 cytochrome b₆f complexes with styrene maleic acid. *Biochim. Biophys. Acta - Bioenerg.* **1859**, 215–225 (2018).
35. Long, A. R. *et al.* A detergent-free strategy for the reconstitution of active enzyme complexes from native biological membranes into nanoscale discs. *BMC Biotechnol.* **13**, 41 (2013).
36. Reading, E. Structural Mass Spectrometry of Membrane Proteins within Their Native Lipid Environments. *Chem. - A Eur. J.* (2018). doi:10.1002/chem.201801556
37. Reading, E. *et al.* Interrogating Membrane Protein Conformational Dynamics within Native Lipid Compositions. *Angew. Chemie - Int. Ed.* **56**, 15654–15657 (2017).
38. Bligh, E. . & Dyer, W. . Canadian Journal of Biochemistry and Physiology. *J. Biochem. Physiol.* **37**, 911–917 (1959).
39. Sud, M. *et al.* LMSD: LIPID MAPS structure database. *Nucleic Acids Res.* **35**, 527–532 (2007).
40. Pappas, A. Epidermal surface lipids. *Dermatoendocrinol.* **1**, 72–76 (2009).
41. Bouwstra, J. A. *et al.* Role of ceramide 1 in the molecular organization of the stratum corneum lipids. *J. Lipid Res.* **39**, 186–196 (1998).

42. Hou, N. S. & Taubert, S. Function and regulation of lipid biology in *Caenorhabditis elegans* aging. *Front. Physiol.* **3 MAY**, 1–10 (2012).
43. Abonnenc, M., Qiao, L., Liu, B. & Girault, H. H. Electrochemical Aspects of Electrospray and Laser Desorption/Ionization for Mass Spectrometry. *Annu. Rev. Anal. Chem.* **3**, 231–254 (2010).
44. Orwick, M. C. *et al.* Detergent-free formation and physicochemical characterization of nanosized lipid-polymer complexes: Lipodisq. *Angew. Chemie - Int. Ed.* **51**, 4653–4657 (2012).
45. Orwick-Rydmark, M. *et al.* Detergent-free incorporation of a seven-transmembrane receptor protein into nanosized bilayer lipodisq particles for functional and biophysical studies. *Nano Lett.* **12**, 4687–4692 (2012).
46. TLC solvent systems. Available at: <https://avantilipids.com/tech-support/analytical-procedures/tlc-solvent-systems/>.
47. Fuchs, B., Süß, R. & Schiller, J. An update of MALDI-TOF mass spectrometry in lipid research. *Prog. Lipid Res.* **49**, 450–475 (2010).
48. Magnusson, C. D. & Haraldsson, G. G. Ether lipids. *Chem. Phys. Lipids* **164**, 315–340 (2011).
49. Kage-Nakadai, E. *et al.* Two very long chain fatty acid acyl-CoA synthetase genes, *acs-20* and *acs-22*, have roles in the cuticle surface barrier in *Caenorhabditis elegans*. *PLoS One* **5**, (2010).
50. Watts, J. L. & Ristow, M. Lipid and carbohydrate metabolism in *Caenorhabditis elegans*. *Genetics* **207**, 413–446 (2017).

Supplementary information

6. Material and methods

6.1. SMA polymer hydrolysis

Styrene-maleic anhydride polymer (SMA_{anh}), in a molar ratio of styrene to maleic anhydride of 3:1, was kindly provided by Malvern Cosmeceutics (Great Malvern, UK). The polymer was hydrolysed using a 1M NaOH solution (5% w/v final) (Fisher) at 80-90 °C for 1-2 h, during which the solution changed from cloudy to a transparent yellow colour. 5 M HCl was then added to precipitate the SMA polymer, which was pelleted by centrifugation (2000g, 5 min, RT).

The pellet was re-solubilised in water and was subjected to multiple washing and centrifugation steps (2000g, 5 minutes). Once washed, double distilled water (ddH₂O) was added to the solution and dialysis was performed overnight in order to remove the excess of salt and to adjust the pH. A transparent yellowish SMA solution resulted, which was lyophilized to yield a white powder. ddH₂O water or buffer was added to a final concentration of 125 mg/ml and the pH was adjusted to pH 8.

6.2. Thin layer chromatography

The lipids were spotted onto a TLC silica gel (Merck). Plates were developed with a methanol/chloroform/ammonium hydroxide (65:25:4 v/v/v) solvent mixture [280]. Lipid bands (Fig. SI.1) were visualized by spraying the plates with molybdenum blue (Sigma) and charred at 200°C. Retention factors (R_f) were calculated.



Cerebrosides $R_f=0.88$

PMME lipid $R_f=0.72$

PG (0.6) or Cardiolipin (0.67) lipid $R_f=0.63$

Synthetic Cardiolipin $R_f=0.3$

LPC $R_f=0.24$

No migration, unknown lipids

agmo-1

Figure 1. *Sl. Thin layer chromatography experiments. The agmo-1 lipid extraction is shown here where different concentrations of lipids were spotted on the plate. Lipid headgroups were identified by their retention factors.*